

Radiative Capture of He^3 by $\text{Li}^{7\dagger}$

P. PAUL, S. L. BLATT, AND D. KOHLER

Department of Physics, Stanford University, Stanford, California

(Received 11 September 1964)

A system suitable for detection of high-energy gamma rays produced with low cross sections in the presence of high background counting rate is described. It is applied to a study of radiative capture of He^3 by Li^7 for bombarding energies up to 3.0 MeV. Gamma transitions to the first six states in B^{10} are observed and their energy dependence is measured. The excitation functions at 90° show peaks at 1.1 and 2.2 MeV for the transitions to the ground state and the one at 4.77 MeV, with c.m. widths of less than 500 and 420 keV, respectively. Transitions to the first and fourth excited states show a broad maximum around 1.4 MeV with a c.m. width of less than 600 keV. The cross section for the decay to 4.77 MeV is largest, with $d\sigma/d\Omega$ reaching $5 \mu\text{b}/\text{sr}$ at the 2.2-MeV peak. At some excitation energies asymmetries $Y(0^\circ)/Y(90^\circ)$ are obtained which indicate strong interferences. The peaks are interpreted as resonances and lower limits on $(2J+1)\Gamma_\gamma$ are presented.

I. INTRODUCTION

INVESTIGATIONS of radiative capture reactions have contributed much information concerning the structure of, and reaction mechanisms involved in light nuclei due to the fact that the electromagnetic interaction itself is so thoroughly understood. Most such studies heretofore have been undertaken using single nucleons and, in some cases, alpha particles. Additional entrance channels can be investigated through study of He^3 and deuteron capture. In many cases these reactions produce the final system at high excitation energies, and thus many low-lying states are available for electromagnetic transitions. This approach allows also the study by gamma deexcitation of high-lying resonances previously investigated primarily by particle emission. The nature of such structures, that is, whether they are compound nuclear resonances, Ericson fluctuations,¹ or intermediate resonances ("doorway states")² may be further clarified by such studies. It may also be possible to determine the extent to which cluster configurations are present³ in the capturing and/or final states. In some nuclei, these reactions may allow study of the giant resonance region even with the use of only moderate energy accelerators. Radiative capture reactions in general, including the capture of H^2 or He^3 , may also make it possible to observe giant resonances based on states other than the ground state.

Investigations of these reactions involve a number of severe experimental difficulties, arising primarily from the fact that radiative capture cross sections are typically very small and the gamma-ray energies are high. These difficulties, specifically obtaining a good line shape for rather high-energy gamma rays, good cosmic-ray rejection, and efficient pulse pileup suppression, have been satisfactorily overcome with a detection system which is described below in Sec. II. A series of radiative capture studies in the light nuclei has been

undertaken in this laboratory with that detection system.⁴ The first reaction extensively investigated is the capture of He^3 by Li^7 for He^3 energies up to 3 MeV. The results of this experiment are presented below.

II. GAMMA-RAY DETECTION SYSTEM

In the development of a system for the detection of gamma rays resulting from the radiative capture of He^3 or deuterons, one must be concerned with the fact that the gamma-ray energies are above about 10 MeV and extend to at least 30 MeV. Hence the system response should have a good line shape for high-energy gamma rays, which would allow study of complex spectra. These radiative capture reactions have very small cross sections, typically of the order of $0.1 \mu\text{b}/\text{sr}$, which makes good cosmic-ray rejection important. Background gamma radiation produced by competing reactions, as well as radiative neutron capture, although generally lower in energy than the He^3 or deuteron capture gamma rays, is often several orders of magnitude more intense. This makes efficient pulse pileup rejection mandatory.

Figure 1 shows a schematic of the detection system employed in the present experiment. It consists of a 5-in.-diam by 6-in.-long NaI(Tl) crystal surrounded by a $1\frac{1}{2}$ -in.-thick cylinder of NE 102 plastic scintillator with a $\frac{1}{4}$ -in.-thick front plate of the same material. The NaI(Tl) crystal was mounted on an RCA 7046 photomultiplier tube, while the plastic shield was viewed by two CBS 7818 tubes the outputs of which were summed. The gamma-ray beam was collimated through a conical hole in a 6-in. lead shield; the aperture of the collimator projected onto the back face of the NaI(Tl) cylinder. The entire system was surrounded by 6 in. of lead.

In order to achieve maximum cosmic-ray rejection, the electronics was arranged so that the anticoincidence gate pulses were generated with minimum possible dead

[†] Work supported in part by the U. S. Army Research Office (Durham), the U. S. Office of Naval Research, and the National Science Foundation.

¹ T. Ericson, *Ann. Phys. (N. Y.)* **23**, 390 (1963).

² H. Feshbach, *Ann. Phys. (N. Y.)* **19**, 287 (1962).

³ G. C. Phillips and T. A. Tombrello, *Nucl. Phys.* **19**, 555 (1960).

⁴ This paper gives experimental details for some work previously published in abstracts: D. Kohler and S. M. Austin, *Bull. Am. Phys. Soc.* **8**, 290 (1963); S. L. Blatt and D. Kohler, *ibid.* **8**, 290 (1963); P. Paul, D. Kohler, and S. L. Blatt, *ibid.* **9**, 391 (1964).

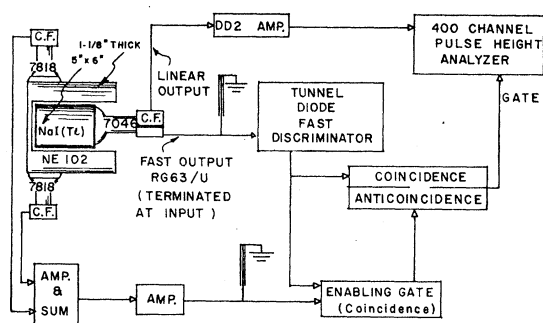


FIG. 1. Setup and electronics block diagram for the gamma-ray detection system. Note that the plastic shield is not drawn to scale.

time. Pulses from the anode of the 7046 were clipped to 25 nsec full width at half-maximum (FWHM) and fed into a tunnel diode discriminator normally biased above the intense low-pulse-height background. This discriminator generated a gate pulse for a Victoreen 400 channel pulse-height analyzer in which the proportional output was stored. At the same time it generated a fast enabling signal for an anticoincidence pulse from the plastic shield, which, only when so enabled, vetoed the pulse-height analyzer gate pulse.

Pileup was reduced by two systems in parallel. The threshold of the fast discriminator could be set to cut out all signals below the region of interest, as mentioned above. This reduced pileup of two small pulses simulating a large one in the linear amplifier by about 40:1, that is the ratio of the 2 μ sec (linear amplifier resolving time) to the 50 nsec (resolving time of the fast discriminator channel). With this suppression, background counting rates 100 times larger than the rates in the region of interest could be tolerated. Pileup of a large pulse with a small one was reduced by an additional, Argonne-type⁵ rejection system which uses fast-coincidence circuitry to measure the time interval between the leading edge and the zero crossing of the double-delay-line-clipped linear pulse. Improvement in the line shape of the main crystal when used with the anticoincidence shield depends on the energy threshold for generating an anticoincidence pulse. In the present system this energy was about 500 keV.

Spectra taken with this detection system showed a reduction in the cosmic-ray background at approximately 15 MeV by a factor of about 70 compared to a system without anticoincidence and lead shielding. Substantial improvement was noted in the gamma-ray line shape, both in resolution and in the reduction of the low-energy tail. Typical line shapes are shown in Fig. 2 for gamma rays between 12 and 20 MeV.

III. EXPERIMENTAL PROCEDURE

Using the detection system described above, the gamma-ray spectrum above 10 MeV resulting from the

⁵ R. E. Segel (private communication).

bombardment of Li^7 with He^3 was measured. The beam was accelerated in the 3-MeV HVEC Van de Graaff at Stanford University. The beam energy was established by magnetic analysis and calibrated with the 874-keV resonance in the reaction $\text{F}^{19}(p,\alpha\gamma)$. Targets were prepared by evaporation in vacuo of 99.7% isotopically enriched Li^7 onto thick copper backings, and were then transferred into the target chamber. The first targets used were covered with a very thin layer of gold to prevent oxidation on transfer. However, since oxygen contamination does not produce gamma rays in the region of interest in reaction with He^3 , the later, thinner ones were allowed to oxidize. Target thickness and uniformity were checked at the 440-keV resonance of the reaction $\text{Li}^7(p,\gamma)$. To keep carbon buildup on the target as low as possible, a liquid-nitrogen trap and a VacIon pump were mounted adjacent to the target chamber. The most intense gamma ray above 12 MeV resulting from He^3 bombardment of carbon is the ground-state transition from the 15.1-MeV state of C^{12} populated⁶ in the reaction $\text{C}^{13}(\text{He}^3,\alpha)\text{C}^{12}$. Using the precautions noted above, the 15.1-MeV gamma-ray inten-

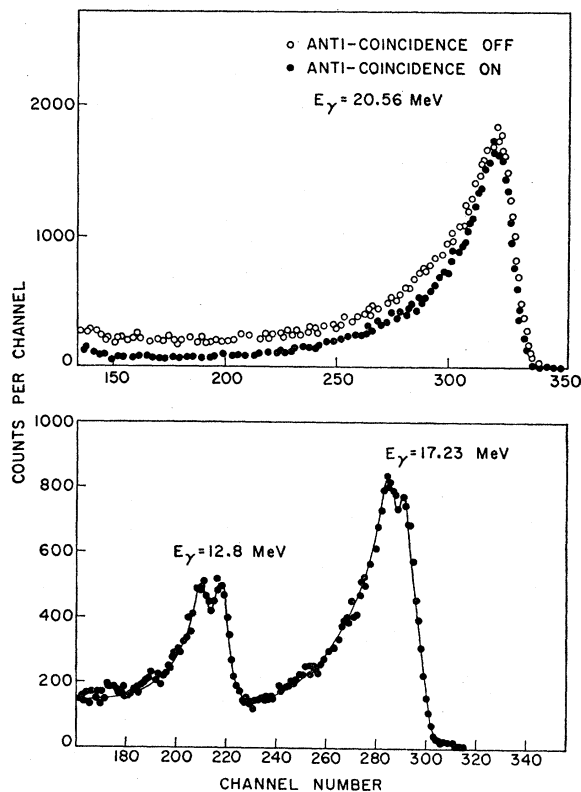


FIG. 2. Gamma-ray spectra obtained with the detection system described in the text. (a) From the reaction $\text{T}(p,\gamma)$ below neutron threshold with and without anticoincidence shield in use. (b) From the reaction $\text{B}^{11}(p,\gamma)$ at $E_p = 1.4$ MeV, showing the transitions to the ground and first excited state in C^{12} , with anticoincidence.

⁶ D. A. Bromley, E. Almquist, H. E. Gove, A. E. Litherland, E. B. Paul, and A. J. Ferguson, *Phys. Rev.* **105**, 957 (1957).

sity present in the experimental spectra appeared to be negligible at all times.

With the detector at 90° to the beam direction, spectra were recorded for He^3 energies from 0.8 to 3.0 MeV in steps of 200 keV, using a target 150 keV thick for 1-MeV He^3 particles. Additional data were taken with a thinner target (50 keV for 1-MeV He^3 particles) from 0.9 to 1.8 MeV in steps of 100 keV. Effects due to slight loss of lithium during bombardment were minimized by measuring each sequence up and down in energy and adding the spectra for each energy. Each run was monitored with the integrated beam current. At some energies, chosen for reasons given in Sec. IV, spectra were also taken at 0° to the beam. Beam currents used were about $1 \mu\text{A}$. With increasing He^3 energy the counting rate in the main photomultiplier, due largely to the increase of neutron background, rises, and hence strong gain changes can occur. To minimize the effect of these changes, a peak whose energy was measured to be 6.96 MeV and was seen in all spectra was used as a fixed energy standard. The position of this peak in the multichannel analyzer was monitored frequently, and no run was accepted if drift was observed. This peak is thought to arise from the summing of γ cascades⁷ from the 6.96-MeV state in Na^{24} populated by capture of slow neutrons in the NaI crystal. The gamma-ray spectrum arising from proton bombardment of tritium above the (p,n) threshold showing this 6.96-MeV peak, is illustrated in Fig. 3.

IV. DATA ANALYSIS AND RESULTS

A typical spectrum, taken at 1.2 MeV ($\theta=90^\circ$) is shown in Fig. 4. A consistent energy calibration scale could be established by using prominent features in all the 90° data, the 6.96-MeV fixed point, and the zero-energy point. Using line shapes interpolated from the standard shapes obtained with the reactions $\text{B}^{11}(p,\gamma)$ and $\text{T}(p,\gamma)$ shown in Fig. 2, the gamma-ray transitions to the first six states of B^{10} were unpeeled consecutively.

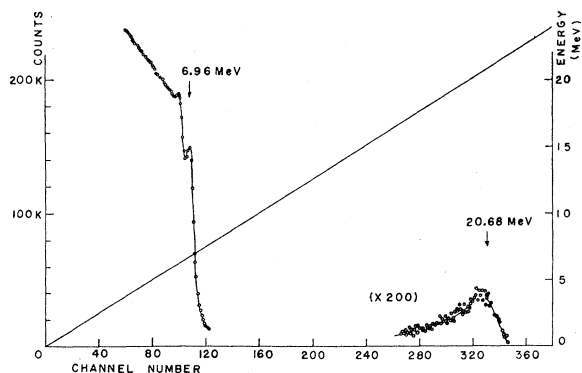


FIG. 3. Gamma-ray spectrum resulting from bombardment of T with p above the neutron threshold, as detected in the NaI crystal. The peak at 6.96 MeV is believed to arise from neutron capture in Na^{23} .

⁷ P. M. Endt and C. Van De Leun, *Nucl. Phys.* **34**, 1 (1962).

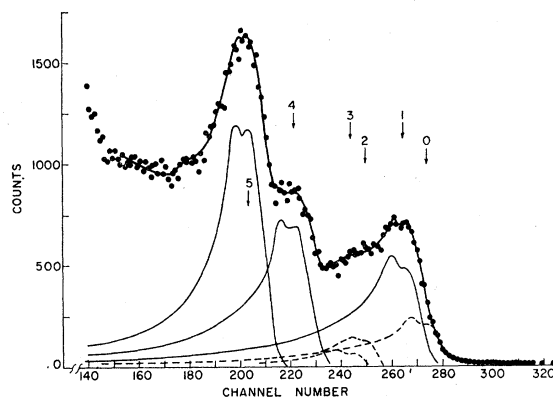


FIG. 4. High-energy part of the gamma-ray spectrum from the reaction $\text{Li}^7(\text{He}^3,\gamma)$ at $E_{\text{He}^3}=1.2$ MeV, obtained at $\theta=90^\circ$. The numerals indicate γ transitions to the ground state and first five excited states in B^{10} .

Figure 5 shows the energetics of the reaction and the observed final states.⁸ The presence of a strong transition to the 4.77-MeV state allows good accuracy up to 5 subtractions. At energies lower than the transition to the 4.77-MeV state there is not enough structure in the spectrum to permit further identification of gamma rays. Gamma rays from the competing $\text{Li}^7(\text{He}^3,\alpha\gamma)$ reaction are expected in this energy region and below, further complicating any attempted analysis. The energies of all the gamma rays identified as originating in radiative capture show the expected dependence on bombarding energy.

For integration of the total counts in each line, the tails were extended horizontally to zero energy. A cross section calibration was obtained with the thicker target and the detection system in the 90° position by using the yield of 17.6-MeV gamma rays produced in the well known⁹ reaction $\text{Li}^7(p,\gamma)$, in the following way. A run was made at the peak of the thick-target excitation curve for the 440-keV resonance. Applying the standard line shape and horizontal tail extension to the 17.6-MeV ground-state transition, the ratio $\sigma(p,\gamma_0)/\sigma(p,\gamma_0+\gamma_1)$ was measured to be 0.59. The close agreement with the known value of 0.63, measured by more accurate means,¹⁰ indicates the subtraction procedure is valid to better than 10%. The differential cross section for $\text{Li}^7(\text{He}^3,\gamma)$ was computed from the relation

$$d\sigma/d\Omega = CY_1/N,$$

where Y_1 is the (He^3,γ) yield, and N is the number of target nuclei/cm². The proportionality constant C for the detection system and target was obtained from the $\text{Li}^7(p,\gamma)$ yield, using the formula

$$C = [d\sigma/d\Omega(\text{res}) \Gamma / (\epsilon Y_2)] \tan^{-1}(\xi/\Gamma),$$

⁸ F. Ajzenberg-Selove and T. Lauritsen, *Nuclear Data Sheets*, compiled by K. Way *et al.* (Printing and Publishing Office, National Academy of Sciences-National Research Council, Washington 25, D. C.), NRC 61-5, 6-91.

⁹ W. Fowler and T. Lauritsen, *Phys. Rev.* **76**, 314 (1949).

¹⁰ M. B. Stearns and B. D. McDaniel, *Phys. Rev.* **82**, 450 (1951).

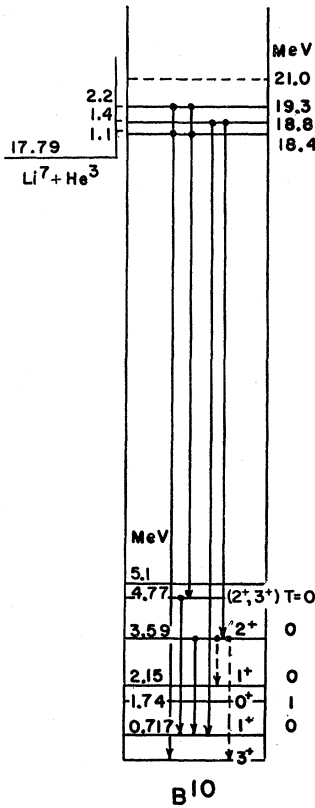


FIG. 5. Simplified level scheme of B^{10} . Vertical arrows are resonant gamma transitions. Horizontal lines above 18 MeV indicate position of resonances observed in the present experiment.

with $d\sigma/d\Omega(\text{res}) = \text{resonance-peak cross section for ground-state transition, } = 0.3 \text{ mb/sr; } \Gamma = \text{total width of 440-keV resonance} = 12 \text{ keV; } \xi = \text{target thickness for 440-keV protons} = 40 \text{ keV; } Y_2 = \text{yield of 17.6-MeV gamma ray. This calibration constant was assumed to be energy independent in the range 13 to 20 MeV. This assumption seems justified for the following reasons: The total detection efficiency of the 5-in.} \times \text{6-in. NaI crystal for the collimated gamma-ray beam changes less than 1.5\% over this range. Additional changes in detection efficiency brought about by energy variation of the anticoincidence rejection ratio are much smaller than errors introduced by the subtraction procedure. The total systematic error on the cross section calibration is estimated to be } \pm 10\%.$

The excitation functions for gamma transitions to the first six states of B^{10} appear as shown in Fig. 6. The error bars are drawn from estimates of maximum and minimum possible subtractions within the spectrum compatible with the assumed line shapes. Open circles refer to the run taken with the 50-keV target. The two separate runs were normalized to account for the different targets but the same factor was used for every transition. The agreement of the two runs at comparable energies is good. All spectra were carefully checked for radiation stemming from the reaction of He^3 with carbon, especially the gamma ray at 15.1 MeV, by comparing spectra taken at the same energies early and late

in a run. The upper limit on the amount of 15.1-MeV gamma ray present is 2% of the counts in this region of the spectrum. This error has been included in the

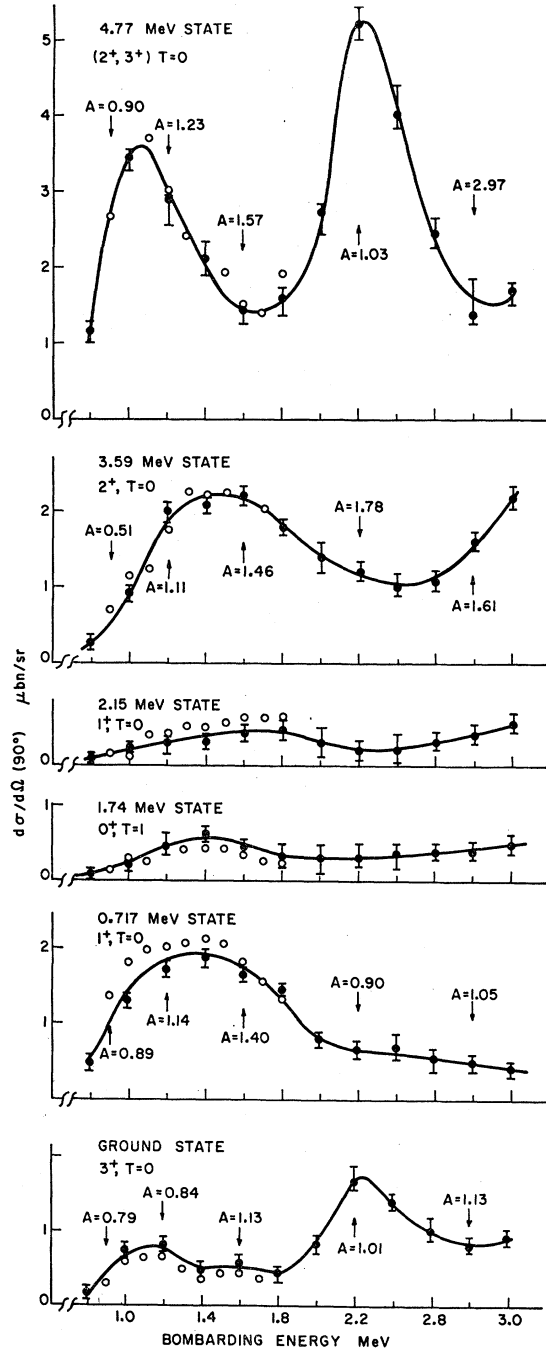


FIG. 6. Excitation functions at 90° of gamma rays observed in $Li^7(He^3, \gamma) B^{10}$. Each curve is marked by the final state in B^{10} and its quantum numbers. Target thickness is 150 keV for 1-MeV He^3 . Open circles represent results from an independent run in 100 keV steps with a target 50-keV thick. A gives the intensity ratio $Y(0^\circ)/Y(90^\circ)$ measured at the indicated energy. Error bars are estimated from the gamma-ray unpeeling procedure. The systematic error on the cross-section scale is $\pm 10\%$.

uncertainties for the transitions to the 3.59- and 4.77-MeV states. At five energies, chosen to be below, on, and above the peaks seen in the 90° excitation functions, runs were also taken at 0°. Figure 6 gives the anisotropy $A = Y(0^\circ)/Y(90^\circ)$ for these energies. The yield in the forward direction was corrected for the absorption of gamma rays in the thick copper backing. Errors in A are $\pm 20\%$.

V. DISCUSSION

The most prominent feature of the data of Fig. 6 are peaks in the cross sections at several energies. The transitions to the ground and 4.77-MeV states show peaks at 1.1 and 2.2 MeV. Those to the 0.72- and 3.59-MeV states show a broad maximum around 1.4 MeV. No finer structure appears in the lower energy region, where data were taken in 100-keV steps with an energy resolution of 50 keV. The most striking peaks are those appearing in the 4.77-MeV state gamma-ray excitation curve. If an s -wave penetration factor is unfolded in the region of the lower peak, which is compatible with the observed isotropy (within the 20% error), the maximum in the cross section shifts to 0.9 MeV. The structure of this excitation function is repeated in the curve for the ground-state transition, most prominently at 2.2 MeV. No peaks appear at these energies in the transitions to the first and fourth excited states, which instead, show a broad maximum at 1.4 MeV. Because of the weakness of the transitions to the second and third excited states and their small separation in energy, the unpeeling of these two gamma rays contains a large uncertainty. The data on these two transitions should not be considered quantitatively reliable, the evidence with respect to them being merely that they are both relatively weak and their excitation functions contain no striking peaks. The data seem to indicate that one or the other or both of them also exhibit the broad peak around 1.4 MeV.

Since these peaks in the cross sections must be related in some way to features in the compound nucleus at high excitation energies, their nature is not trivial to understand. The fact that correlations although limited, appear in the cross sections for different final states apparently excludes an interpretation as Ericson fluctuations.¹ Furthermore, it seems that the peaks should be considered true resonances, either in the usual compound nuclear resonance sense or as intermediate resonances.² In either case they should have definite angular momenta.

The experimentally determined widths of these resonances depend on the background subtraction. For the resonances at 1.1, 1.4, and 2.2 MeV, the limits obtained for the total (c.m.) widths were $\Gamma < 500$ keV, $\Gamma < 600$ keV, and $280 < \Gamma < 420$ keV, respectively. The structure at 1.4 MeV could well consist of two overlapping resonances, although the more detailed run yielded no evidence for this. Figure 5 shows the gamma transitions and excitation energies in B¹⁰ corresponding

to resonances observed in this experiment. Based on the observed strengths of the transitions, it can be assumed¹¹ that transitions slower than electric quadrupole do not contribute. From the decay to final states of different spins,¹² limits on spins and parities of the resonances can be inferred. The spin assignment for the 4.77-MeV state is ambiguous, with 2⁺ and 3⁺ compatible with present experimental evidence.¹³ The possible spin and parity assignments are listed in Table I. Both s -wave and

TABLE I. Resonances observed in radiative capture of He³ by Li⁷.

E_{res} (lab) (MeV)	Γ_{tot} (c.m.) (keV)	Final states in B ¹⁰ (MeV) and their spins	$\frac{d\sigma}{d\Omega}$ (90°) ($\mu\text{b}/\text{sr}$)	Possible spin-parity assignments ^{a,b}	
1.1	<500	0	3 ⁺	0.8	(1 ⁺), 2 [±] , 3 ⁺
		4.77	(2 ⁺ , 3 ⁺)	3.6	
1.4	<600	0.717	1 ⁺	2.0	(0 ⁺), 1 [±] , 2 [±] , (3 ⁺)
		3.59	2 ⁺	2.2	
2.2	280 < Γ < 420	0	3 ⁺	1.8	(1 ⁺), 2 [±] , 3 [±]
		4.77	(2 ⁺ , 3 ⁺)	5.3	

^a Incoming s - and p -waves considered for all resonances; d -waves also considered for 1.4- and 2.2-MeV resonances.

^b Assignments in parentheses require $E2$ transition.

p -wave capture were considered for all resonances, and in addition d -wave capture was included at 1.4 and 2.2 MeV. The experimental anisotropies are of no help in further limiting the spins, since they have large errors and are energy dependent in the vicinity of the resonances. None of the assignments of Table I require anisotropies significantly larger than those obtained experimentally.

If isotropy is assumed the peak differential cross sections for each transition can be used to set a lower limit on the radiative width for the transition using the Breit-Wigner single level formula. Such a lower limit is obtained if Γ_{He^3} is set equal to the total width. The (Be⁷+T) channel, which is expected from charge independence to have the same reduced width as (Li⁷+He³), is open by only 400 keV at the 2.2-MeV resonance, and hence is expected to be much inhibited. A calculation for the transition to the 4.77-MeV state at the 2.2-MeV resonance gives a lower limit of $\Gamma_\gamma = 38$ eV for the highest possible spin, 3. The single-particle Weisskopf estimates¹¹ for this transition are 1000 eV (250 eV with the center-of-mass corrections) for $E1$, 100 eV for $M1$, and 1 eV for $E2$. From the experimental spread for gamma widths in light nuclei, one would expect¹¹ an average width to be 50 eV for $E1$, 10 eV for $M1$, and 10 eV for $E2$. Lower limits for $(2J+1)\Gamma_\gamma$ for all resonant transitions, calculated in the same way, are

¹¹ D. H. Wilkinson, in *Nuclear Spectroscopy*, edited by F. Ajzenberg-Selove (Academic Press Inc., New York, 1960), Vol. B, p. 852.

¹² F. Ajzenberg-Selove and T. Lauritsen, Nucl. Phys. **11**, 1 (1959).

¹³ L. Meyer-Schützmeister and S. S. Hanna, Phys. Rev. **108**, 1506 (1957).

TABLE II. Radiative strengths and He³ single-particle widths estimated for observed resonances in Li⁷(He³, γ).

E_{res} (lab) (MeV)	Γ_{lW} (He ³) ^a = $2P_l(\gamma^2)_W$	Lower limit ^b of $(2J+1)\Gamma_\gamma$ (eV) for transitions to states in B ¹⁰ at					
		$l=0$	$l=1$	$l=2$	0	0.717	3.59
1.1	130	25	1	35	140
1.4	400	100	2	...	100	100	...
2.2	1500	600	50	85	200

^a $(\gamma^2)_W = (3/2)\hbar^2/\mu R^3$, $R = 4.7$ F.

^b Assuming isotropy and $\Gamma_{\text{He}^3} = \Gamma_{\text{tot}}$.

shown in Table II. None of these values are sufficiently outside the known spread in dipole or electric quadrupole widths¹¹ to rule out any of the spin assignments of Table I. For any of the possible spin and parity assignments, however, these radiative widths are quite large, particularly those to the state at 4.77 MeV. Another plausible choice for upper limits on Γ_{He^3} is obtained from the reduced single-particle limit $(\gamma^2)_{\text{He}^3W} = \frac{3}{2}(\hbar^2/\mu R^3)$. The use of these values for s -, p - and d -wave capture yields lower limits for Γ_γ that are generally larger than the one quoted above, especially in the case of d -wave capture, but not by so much as to exclude any of the spin assignments listed in Table I.

VI. CONCLUSION

The specific reaction studied here demonstrates that He³ nuclei can be captured with a sizeable cross section in light nuclei. Although the larger part of the cross section appears to result from resonance capture, it would be interesting to find out how much direct capture could also contribute to the radiative transition strengths. However, this cannot be calculated without detailed knowledge of the nuclear wave functions. A simple model such as the one put forward by Christy and Duck¹⁴ considering only the outer (Coulomb) region of the interaction is not applicable to the present case for the following reason: The main contribution to the matrix element for extranuclear capture is estimated, using Christy and Duck's formula,¹⁴ to originate at a radius of about 1.5 F. This is well inside the nuclear interaction radius of about 4.7 F. The same situation is expected to hold for most high-energy γ rays originating in radiative capture of He³ or deuterons by light nuclei.

The structure observed in the capture cross section apparently corresponds to states in B¹⁰ at excitation energies in the 19-MeV region. The only indication hitherto of such resonances was at $E_{\text{He}^3} = 2.1$ MeV in the reaction¹⁵ Li⁷(He³, α_0)Li⁶. This reaction will be examined in some detail in the paper immediately following.¹⁶ The resonance structure in radiative capture

¹⁴ R. F. Christy and I. Duck, Nucl. Phys. 24, 89 (1961).

¹⁵ E. A. Wolicki and A. R. Knudson, Bull. Am. Phys. Soc. 6, 415 (1961); E. A. Wolicki (private communication).

¹⁶ P. Paul, S. L. Blatt, and D. Kohler, following paper, Phys. Rev. 137, B499 (1965).

is much more pronounced than in the α -particle decay. It might well be generally the case that direct processes are, for the case of multinucleon projectiles, less pronounced in radiative capture than in reactions producing outgoing particles.

The peak cross sections in conjunction with the resonance widths obtained in this experiment, indicate that electromagnetic transitions from the observed resonances to low-lying states in B¹⁰ are strong. Even the lower limits for radiative widths, calculated assuming the largest possible He³ widths, are near the average values found experimentally for dipole transitions, and are large compared to average $E2$ strengths. The radiative widths are thus not expected¹¹ to be larger than these lower limits by more than an order of magnitude. Therefore the He³ widths cannot be expected to be more than an order of magnitude smaller than the values used, which themselves are comparable to, and in most cases even larger than the Wigner single-particle limits. Consequently the (Li⁷+He³) initial state must have good overlap with the states which produce these resonances in B¹⁰. The extreme case would be complete clustering of the observed states into Li⁷+He³. One can then calculate a "single-particle" electromagnetic transition strength, where the radiating particle is now the He³ cluster. In the present case the electric dipole widths so calculated, with the inclusion of c.m. effects, are identical to the values given above for the analogous electric dipole proton single-particle widths.

It is interesting that the strongest observed transitions go to the 4.77-MeV state. This state does not fit well into presently published intermediate coupling shell model calculations,¹⁷ and also shows unusual behavior in its decay modes, being strongly connected by $E2$ to the first excited state¹⁸ but going with an intensity of less than 10% to the ground state. This is not in contradiction to the results of the present experiment, which shows a parallel energy behavior of the transitions to the 4.77 MeV and ground states; if the transitions observed here are of $E1$ character, they are sensitive to the wave functions in a different way than the $E2$ or $M1$ decay modes between the 4.77-MeV state and the lower levels.

The present experiment shows that radiative capture of He³, even at low bombarding energies, can serve as a tool for study of highly excited states in light nuclei. Such results could become more useful when further data on radiative capture of other particles, e.g., protons, in the same region of excitation energy become available.

ACKNOWLEDGMENT

The authors wish to thank N. G. Puttaswamy for his assistance in this experiment.

¹⁷ D. Kurath, *Proceedings of the Rehovoth Conference*, edited by H. I. Lipkin (North-Holland Publishing Company, Amsterdam, 1958), p. 46.